

Electronic Supplement Material (ESI) for Journal of Materials Chemistry C

## Dielectric/SHG/PL triple-channel properties in chiral spirocyclic organic-inorganic hybrids

Xin-Ran Fan,<sup>a</sup> Meng-Meng Lun,<sup>a</sup> Zhi-Jie Wang,<sup>a</sup> Bo-Wen Deng,<sup>a</sup> Da-Wei Fu,<sup>\*a</sup> Chang-Feng Wang,<sup>b</sup> Hai-Feng Lu,<sup>\*b</sup> and Zhi-Xu Zhang<sup>\*b</sup>

<sup>a</sup> Ordered Matter Science Research Center, Jiangsu Key Laboratory for Science and Applications of Molecular Ferroelectrics, Southeast University, Nanjing 211189, People's Republic of China. E-mail: dawei@seu.edu.cn

<sup>b</sup> Institute for Science and Applications of Molecular Ferroelectrics, Key Laboratory of the Ministry of Education for Advanced Catalysis Materials, Zhejiang Normal University, Jinhua 321004, People's Republic of China. E-mail: zhixu@seu.edu.cn

### Experimental Measurement Methods

**Synthesis.** Drugs were purchased directly for use without further purification.

**(*R/S*)-2-hydroxy-5-azaspiro [4.5] decan.** 0.1 mol *R/S*-3-hydroxypyrrolidine hydrochloride and 0.12 mol 1,5-dibromo pentane were dissolved in a mixture of 350 ml of the 2:1 mixture of acetonitrile and methanol, and 0.1 mol potassium carbonate was added as the catalyst. The reactants were poured into a round-bottled flask and stirred. After a reaction of 24 h, the impurities were removed by rotary evaporation to obtain the product *R/S*-2-hydroxy-5-azaspiro [4.5] decan.

**(*R/S*-HASD)<sub>2</sub>MnBr<sub>4</sub>.** 6 mmol *R/S*-HASD was dissolved in 30 ml of the 1:1:1 mixture of water, methanol, and acetonitrile. After dissolving completely, 6 mmol HBr was slowly added dropwise to protonate organic cations. After 2 to 3 minutes, 3 mmol manganese bromide was added, and the mixture was stirred again and placed on a constant temperature heating table at 313 K. After two days, green block crystals were obtained. The specific synthesis route is shown in Fig. S1 (ESI<sup>†</sup>).

**Single-Crystal X-ray Crystallography. (SXR)** The (*R/S*-HASD)<sub>2</sub>MnBr<sub>4</sub> crystal structures were measured using a Rigaku single-crystal X-ray diffractometer with Mo-K $\alpha$  radiation ( $\lambda = 0.71073 \text{ \AA}$ ). Sample structures were determined directly using Olex2 software. The two compounds' specific crystallographic information and structural details are presented in Tables S1 (ESI<sup>†</sup>) and S2(ESI<sup>†</sup>). It is important to note that high-temperature crystal data of plastic phase transitions are difficult to collect with a single crystal diffractometer.<sup>1, 2</sup>

**Dielectric.** The crystals were ground to fine powders and then pressed into 0.35 mm flakes, which were used as electrodes to measure the curve of the dielectric constant  $\epsilon$  as a function of temperature on a Tonhui TH2828A precision instrument. Here,  $\epsilon = \epsilon' + \epsilon''$ , where  $\epsilon''$  is the imaginary part and  $\epsilon'$  is the real part.

**Differential Scanning Calorimetry. (DSC)** The crystals were ground to a fine powder, precisely weighed at 10 mg and loaded into an aluminum crucible, heated and cooled at a rate of 10 K min<sup>-1</sup> over a temperature range from 330-400 K, and DSC curves of both compounds were recorded using a NETZSCH-214 instrument.

**Second harmonic generation. (SHG)** The SHG signals of both compounds were measured using an Edinburgh FLS920 instrument equipped with an Nd: YAG laser ( $\lambda = 1064$  nm, Vibrant 355 II, OPOTEK).

**IR Studies.** IR spectra of two samples in the range of 4000 to 40 cm<sup>-1</sup> were recorded using a Shimadzu-type IR-60 spectrometer at ambient temperature.

**Powder X-ray Diffraction (PXRD) Studies.** X-ray diffraction patterns of the microcrystalline compounds were characterized at room temperature using a Rigaku D/MAX diffraction system under Cu-K $\alpha$  radiation with a diffraction range of 5-50° and a step size of 0.02°. At the same time, the X-ray diffraction patterns of the samples were tested in the temperature range of 298-403 K. In conjunction with the crystallographic information files from the variable temperature X-ray powder diffraction experiments, the space groups of the crystals were simulated using the material studio software package.

**Fluorescence spectroscopy.** The emission and excitation spectra of (R/S-HASD)<sub>2</sub>MnBr<sub>4</sub> were measured using an Edinburgh FLS1000 fluorescence spectrophotometer equipped with a xenon lamp as the excitation source, and time-resolved spectra were recorded through the Edinburgh spectrophotometer equipped with a nanosecond pulsed hydrogen lamp. The temperature range of the multi-temperature fluorescence spectroscopies was 303-413 K. The PLQYs were characterized using an integrating sphere in the spectrofluorometer. The CIE chromaticity coordinates were calculated using the CIE software package based on the emission spectrum data.

**Circular Dichroism (CD).** Circular dichroism spectroscopy (CD) is commonly used to characterize molecular structure and conformation. In this experiment, samples were prepared by the KBr powder and particle compression method, and the CD signals of the two compounds were collected using a JASCO J-810 circular dichroism spectrometer.

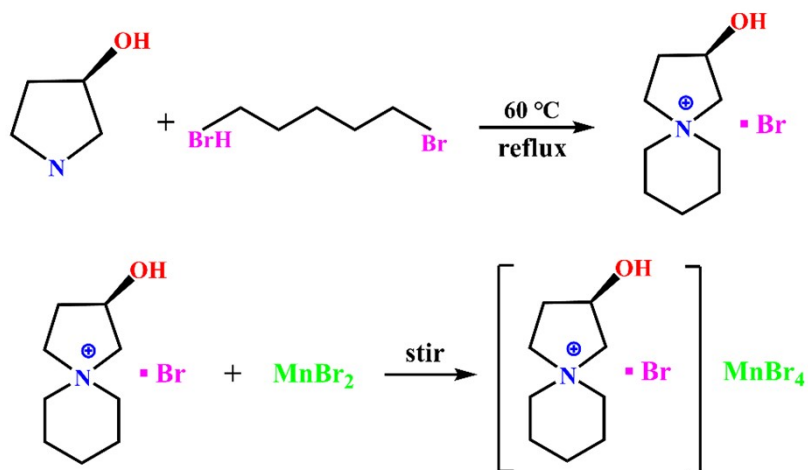


Fig. S1 Specific synthesis route.

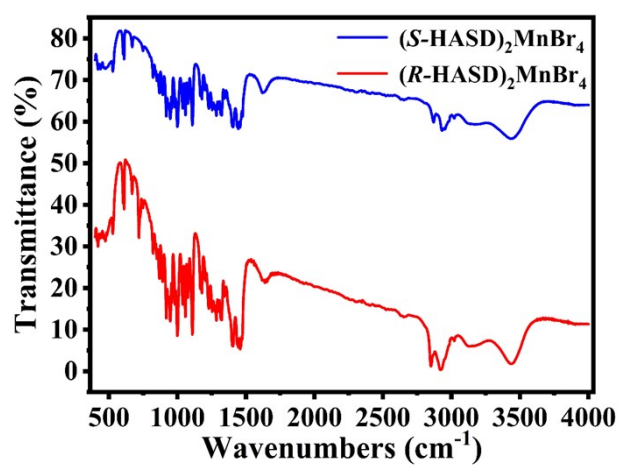


Fig. S2 IR spectra of  $(R/S\text{-HASD})_2\text{MnBr}_4$ .

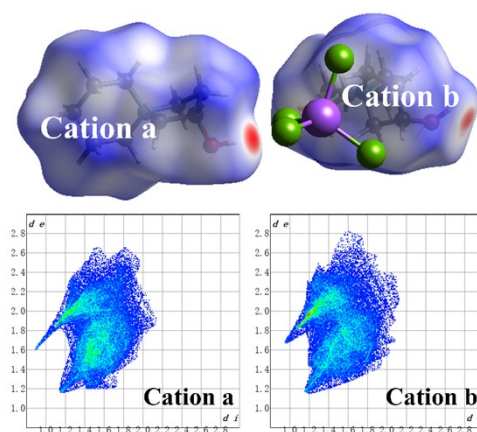
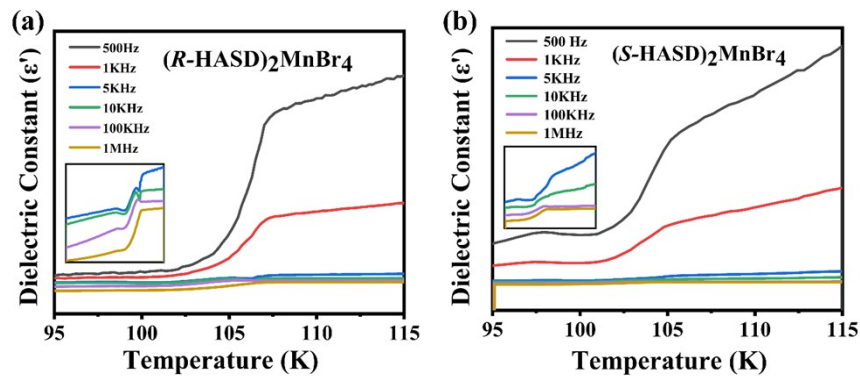
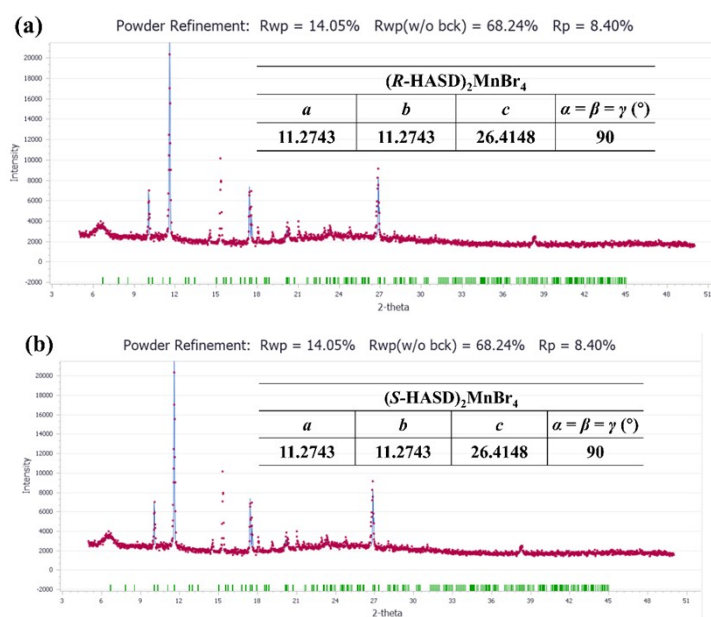


Fig. S3 Hirshfeld  $d_{\text{norm}}$  surface of  $(R\text{-HASD})_2\text{MnBr}_4$  and 2D fingerprint plots of organic cations.



**Fig. S4**  $\epsilon'$  as a function of temperature for  $(R\text{-HASD})_2\text{MnBr}_4$  (a) and  $(S\text{-HASD})_2\text{MnBr}_4$  (b) at different frequencies.



**Fig. S5** Based on the simulation results of PXRD data obtained at 393 K for  $(R\text{-HASD})_2\text{MnBr}_4$  (a) and  $(S\text{-HASD})_2\text{MnBr}_4$  (b) in Material Studio, it is inferred that the HTP of the enantiomer is in tetragonal system, 422 point group, and its space group may be  $I_{41}$ .

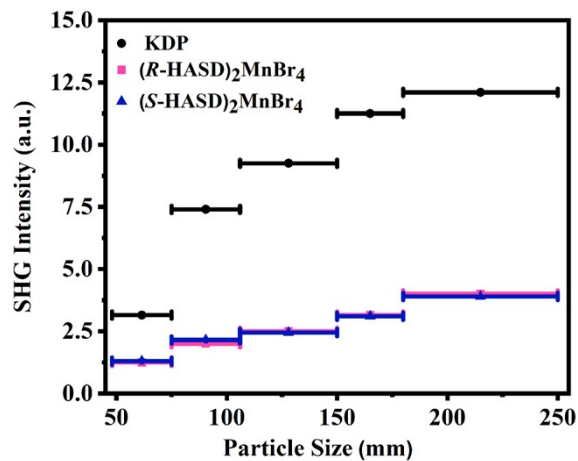


**Fig. S6** Phase matching curve of  $(R\text{-HASD})_2\text{MnBr}_4$  and  $(S\text{-HASD})_2\text{MnBr}_4$  compared with

potassium dihydrogen phosphate (KDP) under 1064 nm laser radiation.

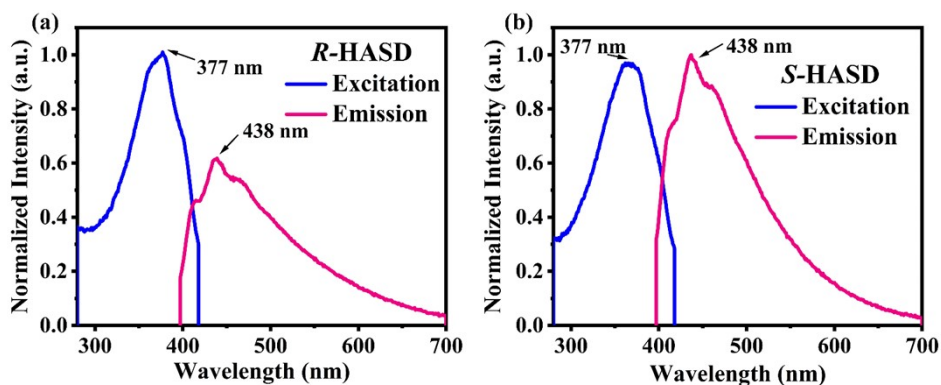


**Fig. S7** Fluorescence spectra of the organic fraction. Excitation and emission spectra of R-HASD (a) and S-HASD (b).

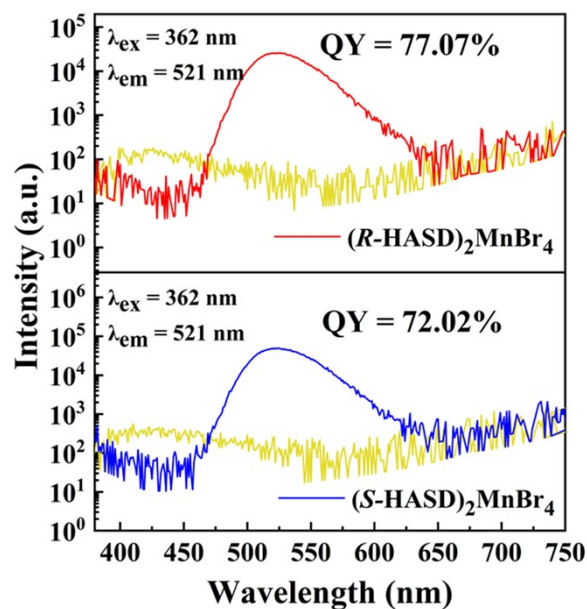


**Fig. S8** PLQYs of  $(R-HASD)_2MnBr_4$  (a) and  $(S-HASD)_2MnBr_4$

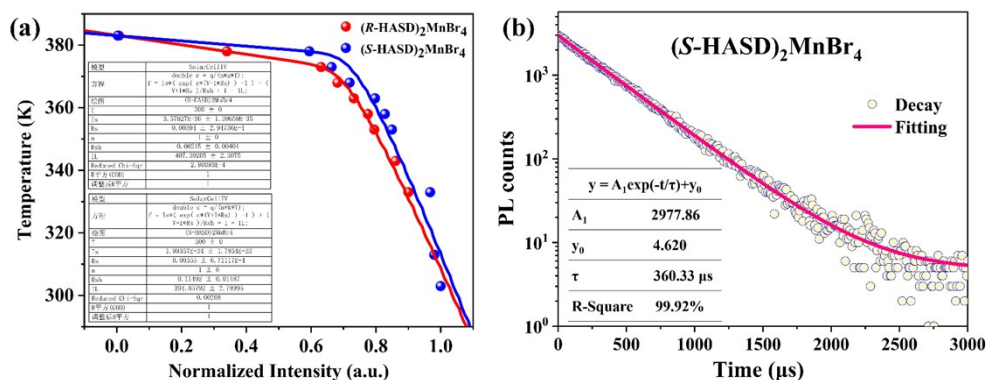


**Fig. S9** (a) PL decay curve of  $(S-HASD)_2MnBr_4$ . (b) The fitted curves of temperature versus PL intensity below  $T_p$ .

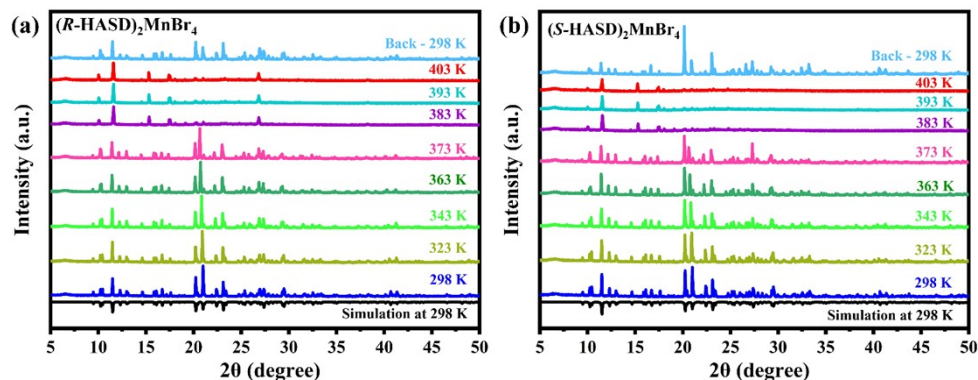


**Fig. S10** PXRD patterns of  $(R\text{-HASD})_2\text{MnBr}_4$  (a) and  $(S\text{-HASD})_2\text{MnBr}_4$  (b) during phase transition.

**Table S1** Crystal data and structure refinement at room temperature.

	$(R\text{-HASD})_2\text{MnBr}_4$	$(S\text{-HASD})_2\text{MnBr}_4$
Empirical formula	$\text{C}_{18}\text{H}_{36}\text{Br}_4\text{MnN}_2\text{O}_2$	$\text{C}_{18}\text{H}_{36}\text{Br}_4\text{MnN}_2\text{O}_2$
Formula weight	687.07	687.07
Temperature/K	298.62(10)	295.42(10)
Crystal system	orthorhombic	orthorhombic
Space group	$P2_12_12_1$	$P2_12_12_1$
$a/\text{\AA}$	11.1465(4)	11.1399(4)
$b/\text{\AA}$	13.6110(7)	13.6053(7)
$c/\text{\AA}$	16.9110(9)	16.9063(9)
$\alpha/^\circ$	90	90
$\beta/^\circ$	90	90
$\gamma/^\circ$	90	90
Volume/ $\text{\AA}^3$	2565.7(2)	2562.4(2)
Z	4	4
F(000)	1356.0	1356.0
Goodness-of-fit on $F^2$	1.018	1.009
$R_1[I \geq 2\sigma(I)]$	0.0442	0.0509
$wR_2[I \geq 2\sigma(I)]$	0.0692	0.1048

**Table S2** Bond Lengths and Bond Angles at room temperature.

Bond Lengths ( $\text{\AA}$ ) and Angles ( $^\circ$ ) for  $(R\text{-HASD})_2\text{MnBr}_4$

Br1-Mn1	2.5008(11)	C12-C13	1.511(10)
Br2-Mn1	2.4875(10)	C10-C14	1.480(10)
Br3-Mn1	2.5179(12)	O1-C8	1.402(8)
Br4-Mn1	2.5130(10)	N1-C9	1.513(7)
N2-C15	1.487(9)	N1-C6	1.547(10)
N2-C18	1.476(8)	N1-C5	1.489(8)
N2-C13	1.504(8)	N1-C1	1.476(12)
N2-C14	1.514(8)	C8-C9	1.516(9)
C15 -C16	1.526(10)	C8-C7	1.460(11)
C17-C16	1.498(12)	C6-C7	1.508(15)
C17 -C18	1.512(11)	C5-C4	1.479(10)
C17 -O2	1.398(9)	C4-C3	1.502(11)
C11-C12	1.509(10)	C1-C2	1.498(15)
C11-C10	1.518(9)	C3-C2	1.498(13)
Br1-Mn1-Br3	109.92(5)	N2-C13-C12	111.6(5)
Br1-Mn1-Br4	109.48(4)	C14 -C10-C11	111.4(6)
Br2-Mn1-Br1	107.68(4)	C10-C14-N2	113.9(6)
Br2-Mn1-Br3	106.45(4)	C9-N1-C6	101.0(5)
Br2-Mn1-Br4	114.29(4)	C5-N1-C9	112.2(5)
Br4-Mn1-Br3	108.93(4)	C5-N1-C6	109.9(6)
C15-N2-C13	110.7(5)	C1-N1-C9	112.1(6)
C15-N2-C14	110.5(6)	C1-N1-C6	112.7(7)
C18 -N2-C15	103.0(5)	C1-N1-C5	108.8(5)
C18 -N2-C13	113.4(5)	O1-C8-C9	107.6(6)
C18 -N2-C14	111.9(5)	O1-C8-C7	113.4(7)
C13 -N2-C14	107.4(5)	C7-C8-C9	106.5(6)
N2-C15-C16	104.4(6)	N1-C9-C8	107.7(5)
C16-C17-C18	105.4(6)	C7-C6-N1	105.9(7)
O2-C17-C16	116.0(9)	C8-C7-C6	100.3(8)
O2-C17-C18	107.7(7)	C4-C5-N1	113.4(6)
C17-C16-C15	105.8(7)	C5-C4-C3	112.1(7)
N2-C18-C17	104.6(6)	N1-C1-C2	112.4(7)
C12 -C11-C10	110.5(6)	C2-C3-C4	108.7(6)
C11-C12-C13	109.7(6)	C1-C2-C3	114.3(9)

Bond Lengths (Å) and Angles (°) for (S-HASD) <sub>2</sub> MnBr <sub>4</sub>			
Br4-Mn1	2.5007(15)	C17-C18	1.51(2)
Br3-Mn1	2.4870(14)	C17 -C16	1.474(18)
Br2-Mn1	2.5176(15)	N1-C5	1.525(10)
Br1-Mn1	2.5130(13)	N1-C7	1.511(12)
C11-C12	1.556(12)	N1-C1	1.509(11)
C11-C10	1.504(16)	N1-C6	1.510(10)
C11-O1	1.405(11)	C5-C4	1.504(14)
N2-C12	1.527(10)	C7-C9	1.573(13)
N2-C14	1.519(10)	O2-C8	1.428(14)
N2-C18	1.469(16)	C4-C3	1.514(15)
N2-C13	1.587(14)	C3-C2	1.568(13)
C10-C13	1.53(2)	C1-C2	1.522(14)
C15-C14	1.500(14)	C9-C8	1.528(17)
C15-C16	1.513(16)	C8-C6	1.539(15)
Br4-Mn1-Br2	109.95(6)	N2-C18-C17	113.2(10)
Br4-Mn1-Br1	109.37(5)	C17-C16-C15	109.0(9)
Br3-Mn1-Br4	107.67(5)	C7-N1-C5	110.3(7)
Br3-Mn1-Br2	106.48(5)	C1-N1-C5	107.7(6)
Br3-Mn1-Br1	114.37(6)	C1-N1-C7	108.7(7)
Br1-Mn1-Br2	108.93(5)	C1-N1-C6	114.2(7)
C10-C11-C12	106.3(8)	C6-N1-C5	111.5(7)
O1-C11-C12	106.4(8)	C6-N1-C7	104.2(7)
O1-C11-C10	113.0(10)	C4-C5-N1	111.1(7)
C12 -N2-C13	102.6(7)	N1-C7-C9	103.3(8)
C14 -N2-C12	112.2(7)	C5-C4-C3	111.2(8)
C14-N2-C13	108.6(8)	C4-C3-C2	108.1(7)
C18-N2-C12	111.5(8)	N1-C1-C2	111.7(8)
C18-N2-C14	108.1(7)	C1-C2-C3	110.5(8)
C18-N2-C13	113.9(10)	C8-C9-C7	105.2(9)
N2-C12-C11	106.8(7)	O2-C8-C9	111.9(12)
C11-C10-C13	100.7(11)	O2-C8-C6	107.5(9)
C14-C15-C16	112.7(10)	C9-C8-C6	106.7(8)

C15-C14-N2	112.2(8)	N1-C6-C8	103.0(8)
C16-C17-C18	112.9(13)	C10-C13-N2	104.5(9)

**Table S3** Enthalpy and Entropy Changes of  $(R\text{-HASD})_2\text{MnBr}_4$  and  $(S\text{-HASD})_2\text{MnBr}_4$  from DSC Data.

	$\Delta H$ (J $\cdot$ mol $^{-1}$ )	$\Delta S$ (J $\cdot$ mol $^{-1}\cdot$ K $^{-1}$ )	$N$
$(R\text{-HASD})_2\text{MnBr}_4$	32.52	58.79	1178
$(S\text{-HASD})_2\text{MnBr}_4$	30.76	55.61	803

## References

1. P. F. Li, W. Q. Liao, Y. Y. Tang, W. Qiao, D. Zhao, Y. Ai, Y. F. Yao and R. G. Xiong, *Proc. Natl. Acad. Sci.*, 2019, **116**, 5878-5885.
2. T. Zhang, S. T. Song, H. N. Zhu, L. L. Chu, D.- W. Fu and Y. Zhang, *Dalton T.*, 2021, **50**, 10142-10146.